Amino Acids (2014) 46:187–198
DOI 10.1007/s00726-013-1616-8

ORIGINAL ARTICLE

Bacterial killing mechanism of sheep myeloid antimicrobial peptide-18 (SMAP-18) and its Trp-substituted analog with improved cell selectivity and reduced mammalian cell toxicity

Binu Jacob · Yangmee Kim · Jae-Kyung Hyun · Il-Seon Park · Jeong-Kyu Bang · Song Yub Shin

Received: 16 August 2013 / Accepted: 25 October 2013 / Published online: 13 November 2013

Abstract To develop short antimicrobial peptide with improved cell selectivity and reduced mammalian cell toxicity compared to sheep myeloid antimicrobial peptide-29 (SMAP-29) and elucidate the possible mechanisms responsible for their antimicrobial action, we synthesized a N-terminal 18-residue peptide amide (SMAP-18) from SMAP-29 and its Trp-substituted analog (SMAP-18-W). Due to their reduced hemolytic activity and retained antimicrobial activity, SMAP-18 and SMAP-18-W showed higher cell selectivity than SMAP-29. In addition, SMAP-18 and SMAP-18-W had no cytotoxicity against three different mammalian cells such as RAW 264.7, NIH-3T3 and HeLa cells even at 100 μM. These results suggest that SMAP-18 and SMAP-18-W have potential for future development as novel therapeutic antimicrobial agent. Unlike SMAP-29, SMAP-18 and SMAP-18-W showed relatively weak ability to induce dye leakage from bacterial membrane-mimicking liposomes, *N*-phenyl-1-napthylamine (NPN) uptake and *o*-nitrophenyl-β-galactoside (ONPG) hydrolysis. Similar to SMAP-29, SMAP-18-W led to a significant membrane depolarization (>80 %) against *Staphylococcus aureus* at 2 × MIC. In contrast, SMAP-18 did not cause any membrane depolarization even at 4 × MIC. In confocal laser scanning microscopy, we observed translocation of SMAP-18 across the membrane in a non-membrane disruptive manner. SMAP-29 and SMAP-18-W were unable to translocate the bacterial membrane. Collectively, we propose here that SMAP-29 and SMAP-18-W kill microorganisms by disrupting/perturbing the lipid bilayer and forming pore/ion channels on bacterial cell membranes, respectively. In contrast, SMAP-18 may kill bacteria via intracellular-targeting mechanism.

Keywords SMAP-18 · Trp-substituted SMAP-18 analog · Cell selectivity · Mammalian cell toxicity · Bacterial killing mechanism

Abbreviations

AMP	Antimicrobial peptide
Fmoc	9-Fluorenylmethoxycarbonyl
TFA	Tifluoroacetic acid
DCC	Dicyclohexylcarbodiimide
HOBt	1-Hydroxy-benzotriazole
$DiSC_3$-5	3,3′-Dipropylthiadicarbocyanine iodide
EYPE	Egg yolk L-α-phosphatidylethanolamine
EYPG	Egg yolk L-α-phosphatidylglycerol
EYPC	Egg yolk L-α-phosphatidylcholine
NPN	*N*-phenyl-1-napthylamine
ONPG	*o*-Nitrophenyl-β-galactoside
FBS	Fetal bovine serum

B. Jacob · I.-S. Park · S. Y. Shin (✉)
Department of Bio-Materials, Graduate School and Department of Cellular and Molecular Medicine, School of Medicine, Chosun University, Gwangju 501-759, Republic of Korea
e-mail: syshin@chosun.ac.kr

Y. Kim
Department of Bioscience and Biotechnology, Bio/Molecular Informatics Center, Konkuk University, Seoul 143-701, Republic of Korea

J.-K. Hyun
Division of Electron Microscopic Research, Korea Basic Science Institute, 113 Gwahanno, Daejeon 305-333, Republic of Korea

J.-K. Bang (✉)
Division of Magnetic Resonance, Korea Basic Science Institute, 804-1 Yangchung-ri, Ochang, Chungbuk 363-883, Republic of Korea
e-mail: bangjk@kbsi.re.kr

MALDI-TOF MS	Matrix-assisted laser desorption ionization–time-of-flight mass spectrometry
RP-HPLC	Reverse-phase high-performance liquid chromatography
CFU	Colony forming unit
MIC	Minimal inhibitory concentration
PBS	Phosphate-buffered saline
MTT	3-(4,5-Dimethylthiazol-2-yl)-2, 5-diphenyl-2H-tetrazolium
LUVs	Large unilamellar vesicles

Introduction

The cathelicidins are a large family of structurally diverse antimicrobial peptides (AMPs) found in mammalian species including humans (Turner et al. 1998; Gennaro and Zanetti 2000). All members of the cathelicidin family contain a N-terminal cathelin domain and a C-terminal domain of varied structure that displays antimicrobial activity after being freed by proteolytic processing of the holoprotein (Travis et al. 2000; Zanetti et al. 1995). Among these, sheep myeloid antimicrobial peptide-29 (SMAP-29) is a 28-residue α-helical cathelicidin-derived AMP with an amidated C-terminus (Bagella et al. 1995). Another form of SMAP-29 also exists which is having 29-residue and non-amidated carboxyl terminal (Dawson and Liu 2009). In this study, 28-residue amidated peptide will be referred as SMAP-29. SMAP-29 displays potent and broad-spectrum antimicrobial activity against Gram-negative and Gram-positive bacteria and fungi (Bagella et al. 1995; Dawson and Liu 2009). However, it is also highly cytotoxic both to human red blood cells (hRBCs) and human embryonic kidney (HEK) cells (Skerlavaj et al. 1999). The cytotoxicity against human normal cells of SMAP-29 is a major barrier for developing it into a novel therapeutic antimicrobial agent. The antimicrobial activity of SMAP-29 has been attributed to the N-terminal amphipathic α-helix region (residues 1–18), and the hemolytic activity to the hydrophobic C-terminal region (residues 19–29) (Shin et al. 2001). A number of variants of SMAP-29 have been prepared in an attempt to improve the cell selectivity for pathogenic microorganisms over mammalian cells (Shin et al. 2001; Dawson and Liu 2011).

In this study, therefore, to develop short AMPs with improved cell selectivity and reduced mammalian cell toxicity compared to SMAP-29 and explore the possible mechanisms responsible for their antimicrobial action, we synthesized SMAP-29 (1–18) amide with amidated C-termini (hereafter called SMAP-18) corresponding to N-terminal amphipathic α-helical domain. Previous study had shown that the N-terminal region is responsible for the antimicrobial activity of SMAP-29 (Shin et al. 2001). SMAP-29 has two α-helical regions connected by a hinge region consisting of Gly and Pro. The carboxyl terminal region is more hydrophobic and may be responsible for higher hemolytic activity of SMAP-29. Other studies also showed that analogs of N-terminal region of SMAP-29 showed potent antimicrobial activity with lower hemolytic activity (Dawson and Liu 2009, 2011).

Several studies suggested that AMPs containing Trp display more potent antimicrobial activity than those with either Phe or Tyr. The bulkier Trp side chain may ensure a more efficient interaction with membrane, allowing the peptides to partition in the bilayer interface (Hu et al. 1993; Oh et al. 2000; Park et al. 2002). For this reason, SMAP-18 analog (SMAP-18-W) was designed by replacing Leu, Leu, Ile and Val residues at positions 3, 6, 10 and 14 of SMAP-18 with Trp. The cell selectivity of the peptides was investigated by examining their antimicrobial activity against Gram-positive and Gram-negative bacterial strains and their hemolytic activity against human red blood cells. The cytotoxicity of these peptides against three different types of mammalian cells (mouse macrophage RAW 264.7, mouse fibroblastic NIH-3T3 cells and human cervical carcinoma HeLa cells) was evaluated. Furthermore, to gain insight the mechanism of bacterial killing action of the peptides, we performed fluorescent dye leakage assay, membrane depolarization assay, time-killing kinetics, *N*-phenyl-1-napthylamine (NPN) assay (outer membrane permeability), *o*-nitrophenyl-β-galactoside (ONPG) hydrolysis assay (inner membrane permeability) and confocal laser scanning microscopy.

Materials and methods

Materials

Rink amide 4-methylbenzhydrylamine (MBHA) resin and 9-fluorenylmethoxycarbonyl (Fmoc) amino acids were obtained from Calbiochem-Novabiochem (La Jolla, CA, USA). Other reagents used for peptide synthesis included TFA (Sigma, St. Louis, MO, USA), piperidine (Merck, Darmstadt, Germany), DCC (Fluka, Buchs, Switzerland), HOBT (Aldrich) and DMF (peptide synthesis grade; Biolab). $DiSC_3$-5 was obtained from Molecular Probes (Eugene, OR, USA). EYPE, EYPG, EYPC, cholesterol, gramicidin D, calcein and NPN, ONPG were supplied by Sigma Chemical Co. (St. Louis, MO, USA). DMEM and FBS were supplied by HyClone (SeouLin, Bioscience, Korea). *Escherichia coli* ML-35, a lactose, permease-deficient strain with constitutive cytoplasmic 3-galactosidase activity (lacI $lacZ^+$ lacY), utilized for inner membrane permeability assays, was obtained

Table 1 Amino acid sequences, calculated and observed molecular masses of SMAP-29, SMAP-18 and its analogs

Peptides	Amino acid sequences	Molecular MS	
		Calculated	Measured[a]
SMAP-29	RGLRRLGRKIAHGVKKYGPTVLRIIRIA-NH_2	3,197.9	3,197.3
SMAP-18	RGLRRLGRKIAHGVKKYG-NH_2	2,064.5	2,065.1
SMAP-18-W	RGWRRWGRKWAHGWKKYG-NH_2	2,370.7	2,371.2

[a] Molecular masses were determined by MALDI-TOF–MS

from Prof. Jae Il Kim, School of Life Science, Gwangju Institute of Science and Technology (GIST), Gwangju, Republic of Korea. All other reagents were of analytical grade. The buffers were prepared in double glass-distilled water.

Peptide synthesis

SMAP-29, SMAP-18 and SMAP-18-W shown in Table 1 were synthesized by the standard Fmoc-based solid-phase method on rink amide 4-methylbenzhydrylamine resin (0.54 mmol/g). DCC and HOBt were used as coupling reagents, and tenfold excess Fmoc-amino acids were added during every coupling cycle. After cleavage and deprotection with a mixture of TFA/water/thioanisole/phenol/ethanedithiol/triisopropylsilane (81.5:5:5:5:2.5:1, v/v/v/v/v/v) for 2 h at room temperature, the crude peptide was repeatedly extracted with diethyl ether and purified by RP-HPLC on a preparative Vydac C18 column (20 mm × 250 mm, 300 Å, 15-mm particle size) using an appropriate 0–90 % water/acetonitrile gradient in the presence of 0.05 % TFA. The final purity of the peptides (>95 %) was assessed by RP-HPLC on an analytical Vydac C18 column (4.6 × 250 mm, 300 Å, 5-mm particle size). The molecular mass of synthetic peptides was determined by MALDI-TOF MS (Shimadzu, Kyoto, Japan) (Table 1).

Antimicrobial assay

The antimicrobial activity of the peptides against three Gram-positive bacterial strains and three Gram-negative bacterial strains was examined using the broth microdilution method in sterile 96-well plates. Aliquots (100 µl) of a bacterial suspension at 2×10^6 CFU/ml in 1 % peptone were added to 100 µl of the peptide solution (serial twofold dilutions in 1 % peptone). After incubation for 18–20 h at 37 °C, bacterial growth inhibition was determined by measuring the absorbance at 600 nm with a Microplate Autoreader EL 800 (Bio-Tek Instruments, VT). The minimal inhibitory concentration (MIC) was defined as the lowest peptide concentration that causes 100 % inhibition of microbial growth. Two types of Gram-positive bacteria (*Staphylococcus epidermidis* [KCTC 1917] and *Staphylococcus aureus* [KCTC 1621]) and three types of Gram-negative bacteria (*Escherichia coli* [KCTC 1682], *Pseudomonas aeruginosa* [KCTC 1637] and *Salmonella typhimurium* [KCTC 1926]) were procured from the Korean Collection for Type Cultures (KCTC) at the Korea Research Institute of Bioscience and Biotechnology (KRIBB).

Measurement of hemolytic activity

The hemolytic activity of the peptides was measured as the amount of hemoglobin released by the lysis of human erythrocytes (Stark et al. 2002). Fresh human red blood cells (hRBCs) were centrifuged, washed three times with PBS (35 mM phosphate buffer, 0.15 M NaCl, pH 7.4), dispensed into 96-well plates as 100 µl of 4 % (v/v) hRBC in PBS, and 100 µl of peptide solution was added to each well. Plates were incubated for 1 h at 37 °C, then centrifuged at 1,000×*g* for 5 min. Samples (100 µl) of supernatant were transferred to 96-well plates and hemoglobin release was monitored by measuring absorbance at 414 nm. Zero hemolysis was determined in PBS (A_{PBS}) and 100 % hemolysis was determined in 0.1 % (v/v) Triton X-100 (A_{triton}). The hemolysis percentage hemolysis was calculated as: $\%\ \text{hemolysis} = 100 \times [(A_{sample} - A_{PBS})/(A_{triton} - A_{PBS})]$.

Mammalian cell cultures

RAW 264.7, NIH-3T3 and HeLa cells were purchased from the American Type Culture Collection (Manassas, VA, USA) and cultured in DMEM supplemented with 10 % fetal bovine serum and antibiotic–antimycotic solution (100 units/ml penicillin, 100 µg/ml streptomycin and 25 µg/ml amphotericin B) in 5 % CO_2 at 37 °C. Cultures were passed every 3–5 days, and cells were detached by brief trypsin treatment, and visualized with an inverted microscope.

Cytotoxicity against mammalian cells

Cytotoxicity of peptides against RAW 264.7, NIH-3T3 and HeLa was determined using the MTT proliferation assay as reported previously with minor modifications (Scudiero et al. 1998). The cells were seeded on 96-well microplates at a density of 2×10^4 cells/well in 150 µl DMEM

containing 10 % fetal bovine serum. Plates were incubated for 24 h at 37 °C in 5 % CO_2. Peptide solutions (20 µl) (serial twofold dilutions in DMEM) were added, and the plates further incubated for 2 days. Wells containing cells without peptides served as controls. Subsequently, 20 µl MTT solution (5 mg/ml) was added in each well, and the plates were incubated for a further 4 h at 37 °C. Precipitated MTT formazan was dissolved in 40 µl of 20 % (w/v) SDS containing 0.01 M HCl for 2 h. Absorbance at 570 nm was measured using a microplate ELISA reader (Molecular Devices, Sunnyvale, CA, USA). Cell survival was expressed as a percentage of the ratio of A_{570} of cells treated with peptide to that of cells only.

Dye leakage assay

Calcein-entrapped LUVs composed of EYPE/EYPG (7:3, w/w) and EYPC/cholesterol (10:1, w/w) were prepared by vortexing the dried lipid in dye buffer solution (70 mM calcein, 10 mM Tris, 150 mM NaCl, 0.1 mM EDTA, pH 7.4). The suspension was subjected to 10 frozen–thaw cycles in liquid nitrogen and extruded 21 times through polycarbonate filters (two stacked 100-nm pore size filters) with a LiposoFast extruder (Avestin, Inc., Canada). Untrapped calcein was removed by gel filtration on a Sephadex G-50 column. The concentration of calcein-entrapped LUVs was determined in triplicate by phosphorus analysis (Barlett 1959). Calcein leakage from LUVs was monitored at room temperature by measuring fluorescence intensity at an excitation wavelength of 490 nm and emission wavelength of 520 nm on a model RF-5301PC spectrophotometer. Complete dye release was obtained using 0.1 % Triton X-100.

Membrane depolarization assay

The cytoplasmic membrane depolarization activity of the peptides was measured using the membrane potential sensitive dye, $diSC_3$-5 as previously described (Wu et al. 1999; Friedrich et al. 2000). In brief, *Staphylococcus aureus* (KCTC 1621) grown at 37 °C with agitation to the mid-log phase ($OD_{600} = 0.4$) was harvested by centrifugation. Cells were washed twice with washing buffer (20 mM glucose, 5 mM HEPES, pH 7.4) and resuspended to an OD_{600} of 0.05 in similar buffer. The cell suspension was incubated with 20 nM $diSC_3$-5 until stable reduction of fluorescence was achieved, implying incorporation of the dye into the bacterial membrane. Then, KCl was added to a final concentration of 0.1 M to equilibrate K^+ levels. Membrane depolarization was monitored by recording changes in the intensity of fluorescence emission of the membrane potential-sensitive dye, $diSC_3$-5 (excitation $\lambda = 622$ nm, emission $\lambda = 670$ nm) after peptide addition. The membrane potential was fully dissipated by adding gramicidin D (final concentration of 0.2 nM). The membrane potential dissipating activity of the peptides is calculated as follows:

$$\% \text{ Membrane depolarization } = 100 \times [(F_p - F_0)/(F_g - F_0)]$$

where F_0 denotes the stable fluorescence value after the addition of the $diSC_3$-5 dye, F_p denotes the fluorescence value 5 min after peptide addition, and F_g denotes the fluorescence signal after gramicidin D addition.

NPN uptake assay

The ability of peptides to increase outer membrane permeability of Gram-negative bacteria was determined by measuring incorporation of the fluorescent dye NPN into the outer membrane of *Escherichia coli* (KCTC 1682) as previously described (Loh et al. 1984; Hancock and Farmer 1993; Ono et al. 1987). In brief, *Escherichia coli* cells were suspended to a final concentration of $OD_{600} = 0.05$ in 5 mM HEPES buffer, pH 7.2, containing 5 mM KCN. NPN was added to 3 ml of cells in a quartz cuvette to give a final concentration of 10 µM and the background fluorescence recorded (excitation $\lambda = 350$ nm, emission $\lambda = 420$ nm). Aliquots of peptide were added to the cuvette and fluorescence recorded as a function of time until there was no further increase in fluorescence. As outer membrane permeability is increased by addition of peptide, NPN incorporated into the membrane causes an increase in fluorescence.

ONPG hydrolysis assay

Inner membrane permeability was determined by measurement in *Escherichia coli* ML-35 of β-galactosidase activity using the normally impermeable, chromogenic substrate ONPG as substrate (Lehrer et al. 1989; Skerlavaj et al. 1990). *Escherichia coli* ML-35 were washed in 10 mM sodium phosphate (pH 7.4) containing 100 mM NaCl and resuspended in the same buffer at a final concentration of $OD_{600} = 0.5$ containing 1.5 mM ONPG. The hydrolysis of ONPG to *o*-nitrophenol over time was monitored spectrophotometrically at 405 nm following the addition of peptide samples.

Time-killing kinetics assay

The time-killing kinetics of the peptides was assessed using *E. coli* (KCTC 1682) and *S. aureus* (KCTC 1621), as described in previous studies (Lee et al. 2008; Koh et al. 2013). The initial density of the cultures was approximately 1×10^6 CFU/ml. After 1, 2, 5, 10, 20 or 40 min of exposure

to the peptides at 37 °C, 50 μl aliquots of serial tenfold dilutions (up to 10^{-3}) of the cultures were plated onto Luria–Bertani (LB) agar plates to obtain viability counts. Colonies were counted after incubation for 24 h at 37 °C.

Confocal laser scanning microscopy

Escherichia coli (KCTC 1682) and *Staphylococcus aureus* (KCTC 1621) cells in mid-logarithmic phase were harvested by centrifugation, washed three times with 10 mM phosphate buffer saline, pH 7.4. Bacteria (10^7 CFU/ml) cells were incubated with FITC-labeled peptides (5 μg/ml) at 37 °C for 30 min. After being incubated, the bacterial cells were pelleted down and washed 3 times with 10 mM phosphate buffer saline, pH 7.4 and immobilized on a glass slide. The FITC-labeled peptides were observed with an Olympus FV1000 confocal laser scanning microscope (Japan). Fluorescent images were obtained with a 488-nm band-pass filter for excitation of FITC.

Results

Antimicrobial and hemolytic activities

We examined the antimicrobial activities of the peptides against a representative set of bacterial strains, including three Gram-negative bacteria (*Escherichia coli*, *Pseudomonas aeruginosa* and *Salmonella typhimurium*) and two Gram-positive bacteria (*Staphylococcus epidermidis* and *Staphylococcus aureus*). As shown in Table 2, both SMAP-18 and SMAP-18-W showed a two- or fourfold decreased antimicrobial activity as compared to parental SMAP-29. The cytotoxicity of the peptides to mammalian cells was measured by their hemolytic activity toward human red blood cells (hRBCs) (Fig. 1). For a quantitative measure of the hemolytic activity of the peptides, we introduced the hemolytic concentration (HC_{50}) defined as the lowest peptide concentration that produces 50 % hemolysis (Table 2). SMAP-29 displayed relatively high hemolytic activity with HC_{50} value of 86 μM. However, both SMAP-18 amide and SMAP-18-W amide did not cause hemolysis at the highest concentration tested (400 μM).

Cytotoxicity against mammalian cells

To further look into the toxic activity of these peptides against mammalian cells, the viability against three different types of mammalian cells, the murine macrophage RAW 264.7 and fibroblast NIH-3T3 cells and the human cervical carcinoma HeLa cells, was determined in the presence of these peptides. MTT assay was performed to determine the activity of the mitochondrial dehydrogenase, which ultimately suggests the viability of the cells. The cytotoxicity of each peptide was defined by IC_{50} (the concentration that causes 50 % growth inhibition for each cell lines). SMAP-29 showed relatively strong cytotoxicity (IC_{50} = 16.0–30 μM) against all three different cells (Fig. 2). In contrast, both SMAP-18 and SMAP-18-W displayed no or less cytotoxicity (IC_{50} > 100 μM) against all three different cells even at 100 μM (Fig. 2).

Table 2 Antimicrobial and hemolytic activities and cell selectivity (therapeutic index) of SMAP-29, SMAP-18 and SMAP-18-W

Peptide	Minimal inhibitory concentration (MIC)[a] (μM)					GM[b] (μM)	HC_{50}[c](μM)	TI[d] (HC_{50}/GM)
	Gram-negative bacteria			Gram-positive bacteria				
	E. coli [KCTC 1682]	*P. aeruginosa* [KCTC 1637]	*S. typhimurium* [KCTC 1926]	*S. epidermidis* [KCTC 1917]	*S. aureus* [KCTC 1621]			
SMAP-29	2	2	1	1	1	1.4	86	61.4
SMAP-18	8	8	2	2	4	4.8	>400	>83.3[e]
SMAP-18-W	4	8	2	2	4	4.0	>400	>100.0[e]
LL-37	8	8	4	64	8	18.4	ND	ND
Melittin	4	8	4	4	2	4.4	ND	ND
Vancomycin	32	4	32	32	0.5	20.1	ND	ND

ND not determined

[a] The lowest peptide concentration that causes 100 % inhibition of microbial growth

[b] The geometric mean of MICs (minimal inhibitory concentrations) from five bacterial strains

[c] The lowest peptide concentration that produces 50 % hemolysis

[d] Therapeutic index: the ratio of the HC_{50} (μM) to the GM (μM)

[e] The ">" denotes that there were no HC_{50} values to calculate the TI within the concentration range tested, so the reported values were minimal TI calculated with 400 μM

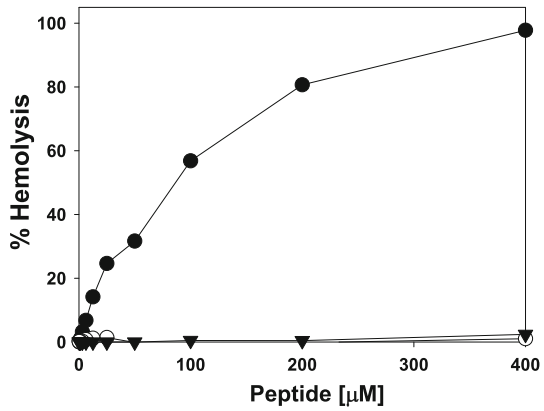

Fig. 1 Concentration–response curves of percent hemolysis of SMAP-29, SMAP-18 and SMAP-18-W against human red blood cells. Symbols: SMAP-29 (*filled circle*), SMAP-18 (*open circle*) and SMAP-18-W (*filled triangle*)

Dye leakage from model membranes

To evaluate the ability of the peptides to permeabilize bacterial and mammalian membranes, we measured their ability to induce leakage of the fluorescent dye calcein from negatively charged EYPE/EYPG (7:3, w/w) LUVs (Fig. 3a, b) and zwitterionic EYPC/cholesterol (10:1, w/w) LUVs (Fig. 3c, d), respectively. SMAP-29 induced a near-complete dye leakage from EYPE/EYPG (7:3, w/w) and EYPC/cholesterol LUVs (10:1, w/w) at 0.5 μM. SMAP-18 induced 11 and 20 % leakage from EYPE/EYPG (7:3, w/w) and EYPC/cholesterol (10:1, w/w) LUVs even at 16 μM, respectively. SMAP-18-W caused 40 % dye leakage from both EYPE/EYPG (7:3, w/w) and EYPC/cholesterol (10:1, w/w) LUVs.

Membrane depolarization

The membrane potential sensitive dye diSC$_3$-5 was used to monitor the cytoplasmic membrane depolarization of *Staphylococcus aureus* cells in the presence of peptides. This dye is distributed between the cells and medium, depending on the cytoplasmic membrane potential, and self-quenches when concentrated inside bacterial cells. If the membrane is depolarized, the probe will be released into the medium, causing a measurable increase in fluorescence. SMAP-29 and SMAP-18-W induced a significant membrane depolarization against *Staphylococcus aureus* in a concentration-dependent manner and depolarized membrane potential of more than 80 % at their 2 × MIC (Fig. 4a). In contrast, SMAP-18 did not cause any membrane depolarization even at 4 × MIC (Fig. 4a). Membrane depolarization was monitored over a period of 550 s for SMAP-29, SMAP-18 and SMAP-18-W (Fig. 4b). SMAP-29 was fast acting, achieving maximum fluorescence at 80 s. The lag time of SMAP-18-W was much longer, leading to maximum fluorescence being achieved after 200 s. The ability of SMAP-29 to depolarize bacterial cells was much greater than that of SMAP-18-W. SMAP-29 induced 100 % membrane depolarization at 2 μM. SMAP-18-W caused approximately 80 % membrane depolarization at 8 μM. In contrast, SMAP-18 did not depolarize the bacterial cytoplasmic membrane even at 16 μM.

Evaluation of outer membrane permeability (NPN uptake)

The ability of the peptides to permeate the outer membrane of *Escherichia coli* was evaluated by the fluorescence-based NPN uptake. NPN is a hydrophobic fluorescent probe that remains quenched in an aqueous environment but fluoresces strongly in a hydrophobic environment. Destabilization of the bacterial outer membrane allows the dye to enter the damaged membrane, where an increase in fluorescence is measured. As observed in LL-37 and melittin, the outer membrane permeabilization of SMAP-29 was detected in a concentration-dependent manner (Fig. 5). In contrast, like to

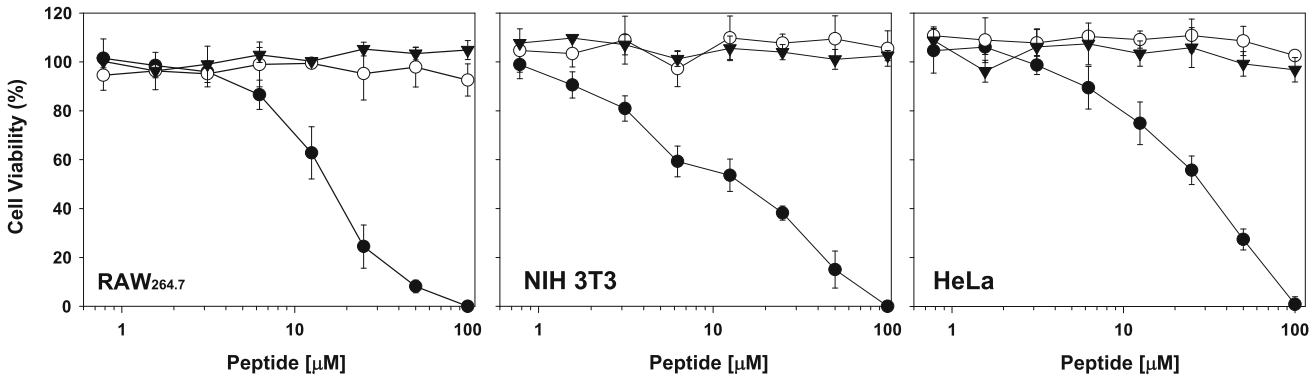

Fig. 2 Cytotoxicity of SMAP-29, SMAP-18 and SMAP-18-W against three different types of mammalian cells, mouse macrophage RAW 264.7 cells, and mouse fibroblast NIH-3T3 cells and human cervical carcinoma HeLa cells. Symbols: SMAP-29 (*filled circle*), SMAP-18 (*open circle*) and SMAP-18-W (*filled triangle*)

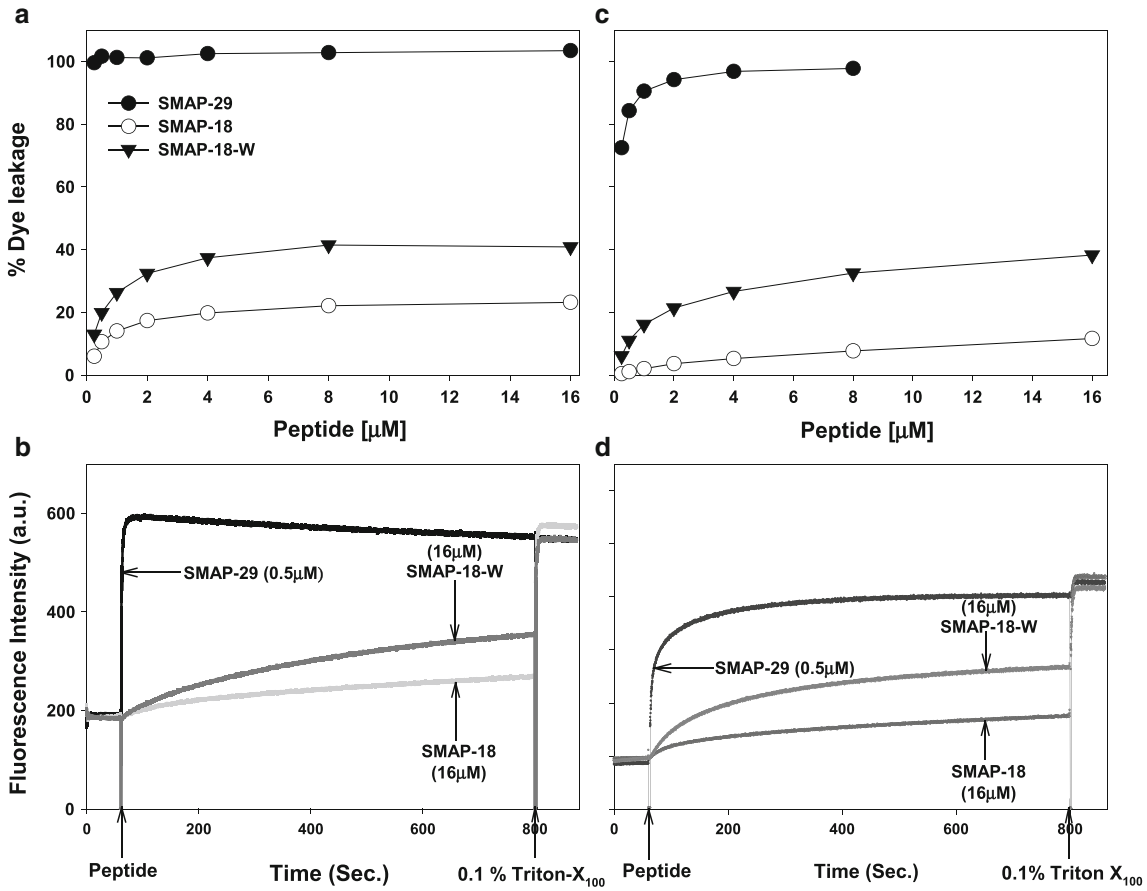

Fig. 3 **a** Concentration-dependent peptide-induced calcein release from calcein-entrapped negatively charged EYPE/EYPG (7:3, w/w) LUVs. Symbols: SMAP-29 (*filled circle*), SMAP-18 (*open circle*) and SMAP-18-W (*filled triangle*). **b** Time-dependent peptide-induced calcein release from calcein-entrapped negatively charged EYPE/EYPG (7:3, w/w) LUVs. **c** Concentration-dependent peptide-induced dye release from calcein-entrapped zwitterionic EYPC/cholesterol (10:1, w/w) LUVs. Symbols: SMAP-29 (*filled circle*), SMAP-18 (*open circle*) and SMAP-18-W (*filled triangle*). **d** Time-dependent peptide-induced dye release from calcein-entrapped zwitterionic EYPC/cholesterol (10:1, w/w)

buforin-2, SMAP-18 and SMAP-18-W induced relatively little NPN uptake even at 16 μM (Fig. 5).

Evaluation of inner membrane permeability (ONPG hydrolysis)

In order to complete membrane permeabilization, peptides translocation to inner membrane is one of the critical steps. Inner membrane permeabilization was indicated by influx of nonchromogenic substrate ONPG that was subsequently cleaved to the yellow product ONP by β-galactosidase in the cytoplasm. As shown in Fig. 6, the inner membrane permeabilization of SMAP-29 was detected in a concentration-dependent manner. SMAP-29 induced inner membrane permeation at a high rate, as reflected in the greater slope of ONPG hydrolysis at 0–80 min. In contrast, SMAP-18 and SMAP-18-W did not induce inner membrane permeation even at 16 μM. Also, LL-37 and buforin-2 (used as reference peptides) caused weak or less inner membrane permeation even at 16 μM.

Time-kill kinetics

To study the bactericidal kinetics of the peptides against Gram-negative and Gram-positive bacteria, time-killing analyses were carried out using *E. coli* (KCTC 1682) and *S. aureus* (KCTC 1621) at 0.5 × MIC. As shown in Fig. 7, SMAP-29 completely killed both Gram-negative and Gram-positive bacteria in less than 2 min. SMAP-18-W was slower than SAMP-29 but killed bacteria faster than SMAP-18. SMAP-18 took longest time among all peptides.

Confocal laser scanning microscopy

To investigate the action site of SMAP-29, SMAP-18 and SMAP-18-W, their FITC-labeled peptides was incubated

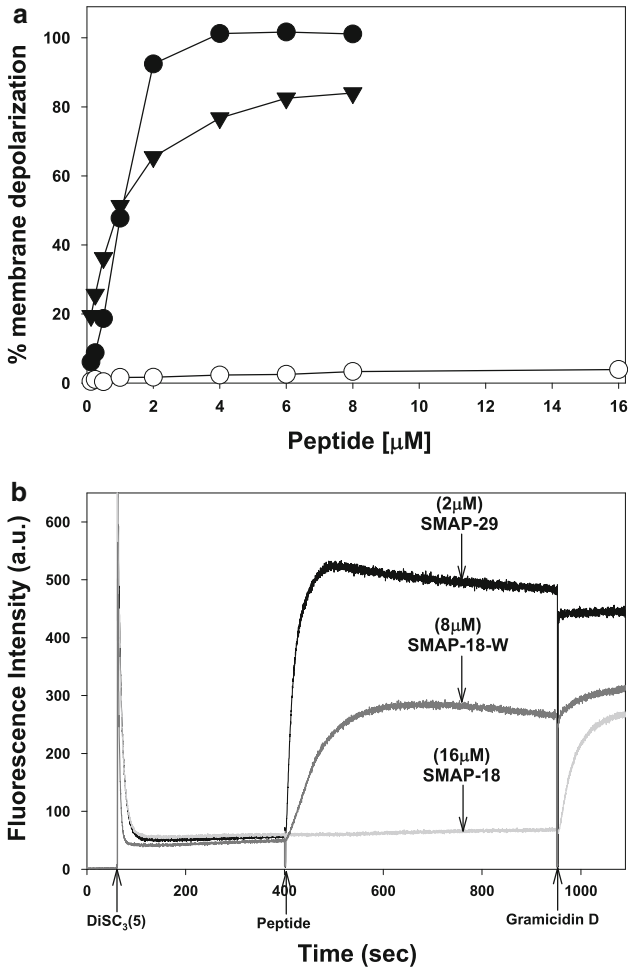

Fig. 4 **a** Concentration-dependent membrane depolarization of *Staphylococcus aureus* by SMAP-29, SMAP-18 and SMAP-18-W. Symbols: SMAP-29 (*filled circle*), SMAP-18 (*open circle*) and SMAP-18-W (*filled triangle*). **b** Time-dependent membrane depolarization of *Staphylococcus aureus* by SMAP-29 (2 μM), SMAP-18 (16 μM) and SMAP-18-W (8 μM)

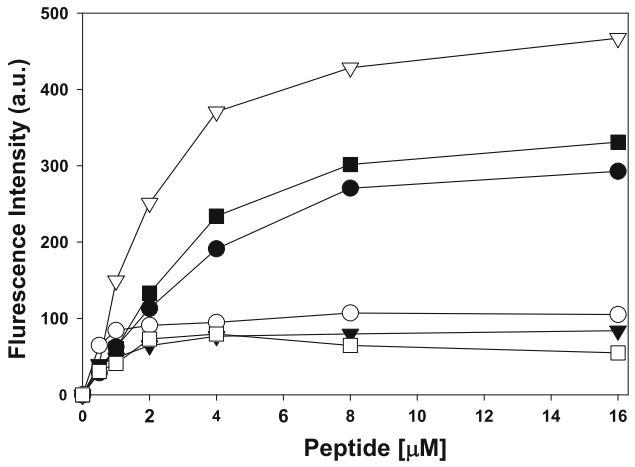

Fig. 5 Peptide-mediated NPN uptake in *Escherichia coli*. *E. coli* cells were incubated with NPN in the presence of various concentrations of the peptides. Enhanced uptake of NPN was measured by an increase in fluorescence caused by partitioning of NPN into the hydrophobic interior of the outer membrane. Symbols: SMAP-29 (*filled circle*), SMAP-18 (*open circle*), SMAP-18-W (*filled triangle*). LL-37 (*open triangle*), melittin (*filled square*) and buforin-2 (*open square*)

with log-phase *Escherichia coli* and *Staphylococcus aureus* and their localization was visualized by confocal laser scanning microscopy (Fig. 8). Bacterial cells treated for half an hour with FITC-labeled SMAP-18 and buforin-2 at room temperature appeared as green rods with fluorescence spread throughout the bacterial cell indicating the internalization of FITC-labeled peptide into the cytoplasm of the bacteria. In contrast, the internalization of FITC-labeled peptide into the cytoplasm of the bacteria was not found in SMAP-29 and SMAP-18-W.

Discussion

The therapeutic potential of AMPs lies in the cell selectivity for bacteria over human erythrocytes. Cell selectivity is a measure of peptide's capability to differentiate any pathogen against host cells. It is one of the most difficult challenges in the development of antimicrobial agents, especially if the target of action is cytoplasmic membrane. The cell selectivity of the peptides is defined by the concept of the therapeutic index (TI) as a measure of the relative safety of the drug (Chen et al. 2005; Fázio et al. 2007; Park et al. 2008, 2009; Solanas et al. 2009; Nan et al. 2012). Larger values of TI indicate greater cell selectivity. The TI of each peptide was calculated as the ratio of the HC_{50} (the peptide concentration needed to reach 50 % lysis of human red blood cells) value to the GM (geometric mean of MICs against five microorganisms) ($TI = HC_{50}/GM$). As shown in Table 2, SMAP-18 and SMAP-18-W showed higher TI than SMAP-29. In addition to hemolytic activity toward human erythrocytes, the cytotoxicity of the peptides against three mammalian cells including NIH-3T3 fibroblasts, HeLa and RAW264.7 cells was evaluated. Unlike SMAP-29, SMAP-18 and SMAP-18-W were not cytotoxic up to 100 μM. These results suggest that SMAP-18 and SMAP-18-W are promising candidates for novel therapeutic antimicrobial agents, complementing conventional antibiotic therapies to combat pathogenic microorganisms.

Bacterial killing effect of the majority of AMPs such as LL-37, melittin and SMAP-29 is considered to be due to their action on the lipid matrix of bacterial cell membranes, either by forming pore/ion channels or disrupting the bilayer (i.e. membrane-targeting AMPs) (Matsuzaki 1998; Oren and Shai 1998; Heller et al. 2000). These membrane-targeting AMPs were reported to act mainly by causing membrane lysis either by barrel stave, toroidal

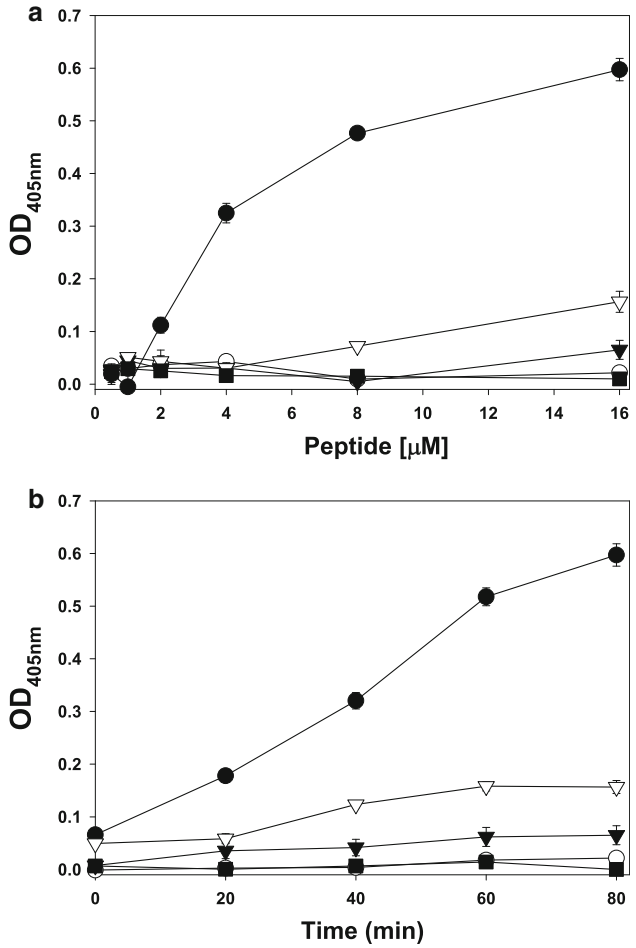

Fig. 6 Peptide-mediated inner membrane permeabilization of *Escherichia coli* ML-35. Permeabilization was determined by following spectrophotometrically at 420 nm, the unmasking of cytoplasmic β-galactosidase activity as assessed by hydrolysis of the normally impermeable, chromogenic substrate ONPG. *E. coli* (approximately 10^6 colony forming units/ml) were resuspended in 10 mM sodium phosphate buffer, pH 7.5, containing 100 mM NaCl and 1.5 mM substrate. Symbols: SMAP-29 (*filled circle*), SMAP-18 (*open circle*), SMAP-18-W (*filled triangle*), LL-37 (*open triangle*) and buforin-2 (*filled square*)

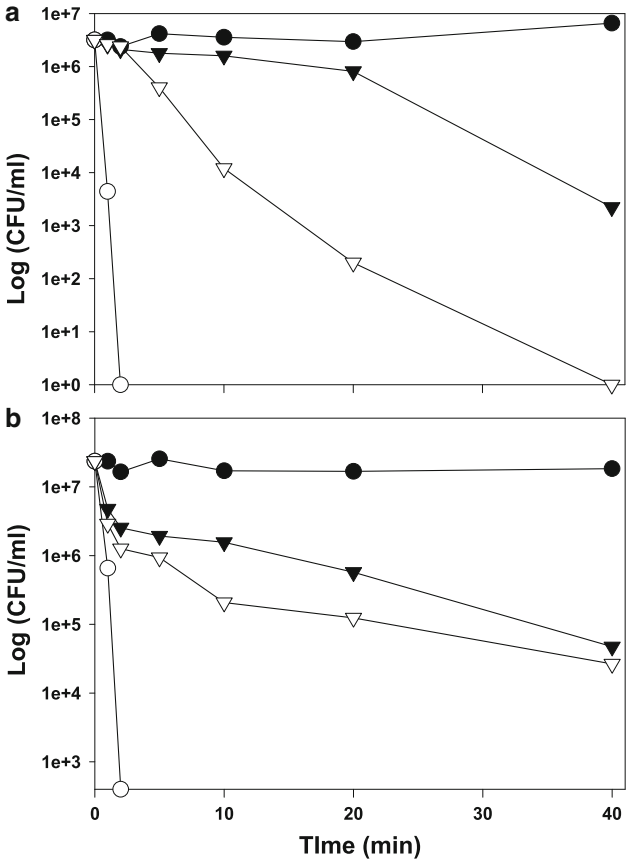

Fig. 7 Time-kill kinetics of *Escherichia coli* (**a**) and *Staphylococcus aureus* (**b**) treated with the peptides at 0.5 × MIC. Symbols: without peptide (*filled circle*), SMAP-29 (*open circle*), SMAP-18 (*filled triangle*) and SMAP-18-W (*open triangle*)

pore or carpet-like mechanisms (Giuliani et al. 2008; Nguyen et al. 2011; Sato and Feix 2006). No single mechanism can be defined for all peptides (Zhang et al. 2001). Furthermore, membrane disruption mechanisms for a given peptide can vary depending on lipid composition or other environmental conditions, for example melittin and aurein were found to act by three different mechanisms depending on the conditions used (Zhang et al. 2001; Allende et al. 2005; Cheng et al. 2009; Ladokhin and White 2001; Wiedman et al. 2013). In contrast, a few AMPs such as buforin 2 and PR-39 were known to penetrate microbial cell membranes without inducing membrane permeabilization and cause bacterial cell death by inhibiting protein, DNA or RNA synthesis (i.e. intracellular-targeting AMPs) (Park et al. 1998, 2000; Kobayashi et al. 2004; Song et al. 2005).

To examine whether the cytoplasmic membrane of bacterial cells is the ultimate target of SMAP-18 and SMAP-18-W and to determine their membrane selectivity, the abilities of these peptides to cause leakage of a fluorescent dye entrapped within LUVs composed of negatively charged EYPE/EYPG (7:3, w/w) was tested. SMAP-29 showed very strong dye leakage from bacterial membrane-mimicking lipid vesicles as melittin does. In contrast, SMAP-18 and SMAP-18-W caused a 20 and 40 % leakage from calcein-entrapped negatively charged EYPG/EYPE (7:3, w/w) at 16 μM, respectively. Also, SMAP-29 induced very strong dye leakage from mammalian membrane-mimetic EYPC/cholesterol (10:1, w/w) liposome, but SMAP-18 and SMAP-18-W displayed 11 and 40 % dye leakage. These results suggested that SMAP-18 is more selective to bacterial membranes as compared to SMAP-29 and SMAP-18-W.

Next, we measured the effects of the peptides on bacterial membrane potential in *Staphylococcus aureus* using a

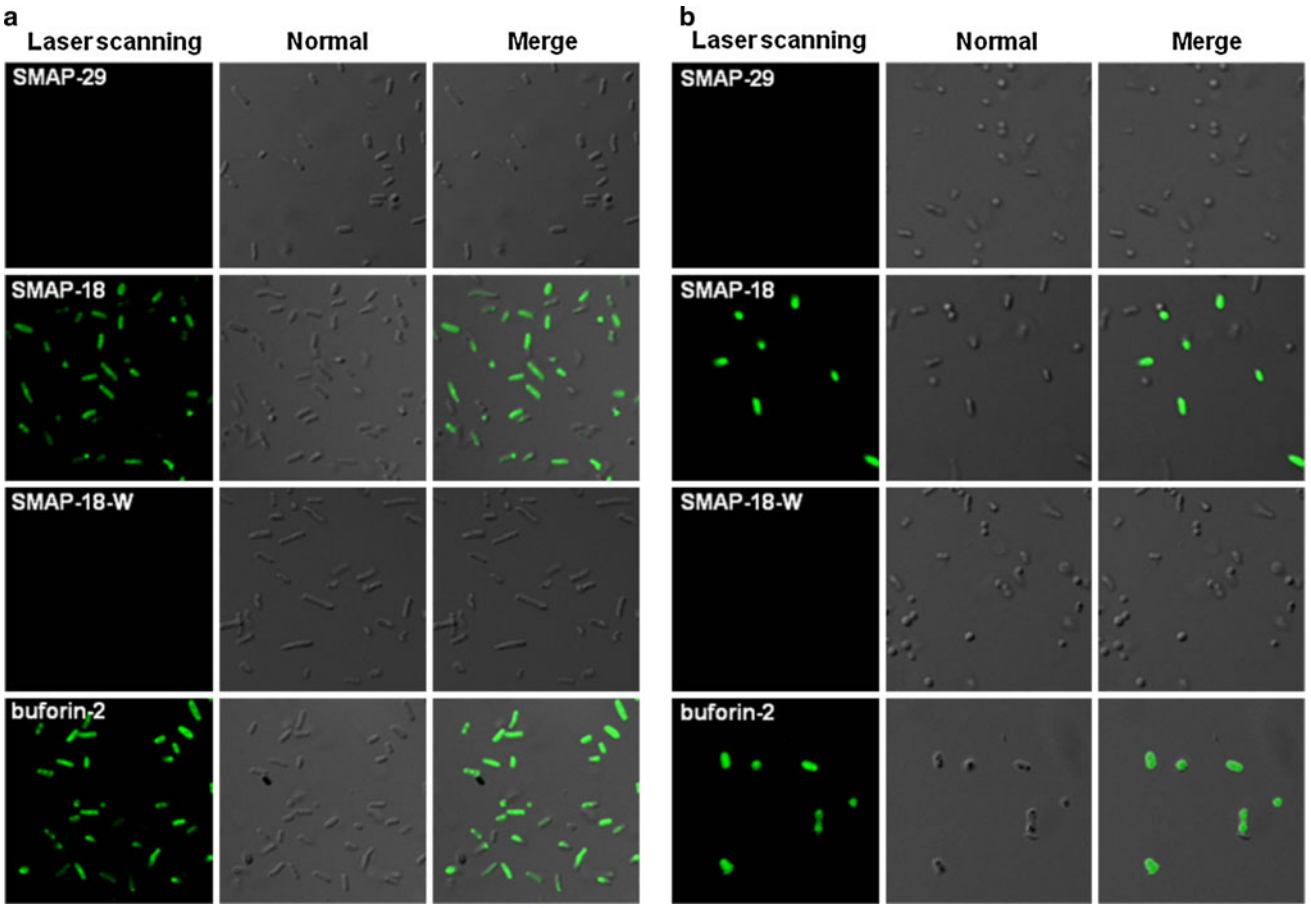

Fig. 8 Confocal laser scanning microscopy of *Escherichia coli* (KCTC 1682) or *Staphylococcus aureus* (KCTC 1621) treated with FITC-labeled peptides. The cells were incubated with FITC-labeled peptides (5 μg/ml) at 37 °C for 30 min. Panels on the *left*, *middle* and *right* represent laser-scanning images, transmitted light scanning image (normal image), and merged image of *E. coli* (A) and *S. aureus* (B) respectively, treated with FITC-labeled peptides

membrane potential sensitive dye, $diSC_3$-5. The $diSC_3$-5 release assay indicated the peptides ability to disrupt the membrane potential across the cytoplasmic membrane. SMAP-29 and SMAP-18-W induced a significant membrane depolarization at 1 or 2 × MIC. In contrast, SMAP-18 caused no membrane depolarization even at 4 × MIC. Our previous study, buforin-2 also induced less or no membrane depolarization even at 4 × MIC (Zhu et al. 2009). This high membrane depolarization ability of SMAP-18-W is not extended to ability to induce calcein leakage from LUVs. This may be due to the reason that SMAP-18-W could form pores on the membrane which could only allow small ions not large molecules such as calcein.

The ability of the peptides to permeabilize the outer membrane was observed using NPN uptake on *E. coli*. Increase in NPN fluorescence was due to outer membrane disintegration from peptide permeabilization. Like LL-37 and melittin, SMAP-29 was able to induce NPN uptake. However, SMAP-18 and SMAP-18-W induced relatively little NPN uptake even at 16 μM. Furthermore, the potential of inner membrane permeation of the peptides was evaluated by ONPG hydrolysis assay. Interestingly, the inner membrane permeabilizing activity of SMAP-29 is considerably higher than that of other membrane-targeting AMPs such as LL-37. However, SMAP-18 and SMAP-18-W did not induce inner membrane permeation even at 16 μM. The membrane-targeting AMPs in general have faster time-kill kinetics compared to intracellular-targeting AMPs. The time-killing kinetics of SMAP-29, SMAP-18 and SMAP-18-W was carried out using *E. coli* and *S. aureus* to compare the time taken to kill bacteria. The fast kinetics of SMAP-29 and SMAP-18-W compared to SMAP-18 indicated that their target is bacterial membrane. On the contrary, the slow kinetics of SMAP-18 suggested that it has a different mode of interaction with the lipid bilayer. The slower killing of SMAP-18 may be due to its plausible intracellular targets.

For the determination of site of action of the peptides, FITC-labeled peptides were incubated with log-phase

E. coli and their localization was visualized by confocal laser-scanning microscopy. Like buforin-2, it was observed that SMAP-18 was able to traverse bacterial membrane along with cell damage. This finding indicates that the major site of action of SMAP-18 is the cytoplasm of bacteria. In contrast, SMAP-29 and SMAP-18-W were unable to translocate the bacterial membrane.

The structure of SMAP-29 has three segments; the flexible N-terminal region, a hinge of Gly, nearly α-helical segment of Arg 8 to Tyr 17, another hinge of glycine and proline, and α-helix-like carboxy-terminal region (Tack et al. 2002). A previous study had shown that the removal of second hinge region and carboxy-terminal region will significantly reduce the hemolytic activity (Shin et al. 2001). It suggests that the membrane interaction is due to carboxy-terminal region following the initial electrostatic interaction of N-terminal region.

On the other hand, SMAP-18 lacks the hinge and second helix-like region, thus unable to disrupt the membrane immediately as its parent peptide SMAP-29. Other studies had shown that the derivatives of SMAP-18 have amphipathic α-helical structure (Sawai et al. 2002). Amphipathic α-helical peptides that are rich in Arg and Leu were shown to have cell penetrating abilities without pore formation (Walrant et al. 2012; Derossi et al. 1998). Thus, it is possible that SMAP-18 has a unique cell penetrating property across the membrane and killing bacteria by acting on intracellular targets.

Based on these results, we propose here that SMAP-29 and SMAP-18-W kill microorganisms by disrupting/perturbing the lipid bilayer (carpet-like model) and forming pore/ion channels on bacterial cell membranes (barrel stave model or toroidal model), respectively. In contrast, the bacterial killing by SMAP-18 may due to the inhibition of the intracellular functions (e.g. DNA, RNA or protein).

Conflict of interest The authors have declared that there is no conflict of interest.

References

Allende D, Simon SA, McIntosh TJ (2005) Melittin-induced bilayer leakage depends on lipid material properties: evidence for toroidal pores. Biophys J 88:1828–1837

Bagella L, Scocchi M, Zanetti M (1995) cDNA sequences of the three sheep myeloid cathelicidins. FEBS Lett 376:225–228

Barlett GR (1959) Phosphorus assay in column chromatography. J Biol Chem 234:466–468

Chen Y, Mant CT, Farmer SW, Hancock RE, Vasil ML, Hodges RS (2005) Rational design of α-helical antimicrobial peptides with enhanced activities and specificity/therapeutic index. J Biol Chem 280:12316–12329

Cheng JT, Hale JD, Elliot M, Hancock RE, Straus SK (2009) Effect of membrane composition on antimicrobial peptides aurein 2.2 and 2.3 from Australian southern bell frogs. Biophys J 96:552–565

Dawson RM, Liu CQ (2009) Cathelicidin peptide SMAP-29: comprehensive review of its properties and potential as a novel class of antibiotics. Drug Dev Res 70:481–498

Dawson RM, Liu CQ (2011) Analogues of peptide SMAP-29 with comparable antimicrobial potency and reduced cytotoxicity. Int J Antimicrob Agents 37:432–437

Derossi D, Chassaing G, Prochiantz A (1998) Trojan peptides: the penetratin system for intracellular delivery. Trends Cell Biol 8:84–87

Fázio MA, Jouvensal L, Vovelle F, Bulet P, Miranda MT, Daffre S, Miranda A (2007) Biological and structural characterization of new linear gomesin analogues with improved therapeutic indices. Biopolymers 88:386–400

Friedrich CL, Moyles D, Beveridge TJ, Hancock RE (2000) Antibacterial action of structurally diverse cationic peptides on gram-positive bacteria. Antimicrob Agents Chemother 44:2086–2092

Gennaro R, Zanetti M (2000) Structural features and biological activities of the cathelicidin-derived antimicrobial peptides. Biopolymers 55:31–49

Giuliani A, Pirri G, Bozzi A, Giulio A, Aschi M, Rinaldi AC (2008) Antimicrobial peptides: natural templates for synthetic membrane-active compounds. Cell Mol Life Sci 65:2450–2460

Hancock RE, Farmer SW (1993) Mechanism of uptake of deglucoteicoplanin amide derivatives across outer membranes of *Escherichia coli* and *Pseudomonas aeruginosa*. Antimicrob Agents Chemother 37:453–456

Heller WT, Waring AJ, Lehrer RI, Harroun TA, Weiss TM, Yang L, Huang HW (2000) Membrane thinning effect of the β-sheet antimicrobial protegrin. Biochemistry 39:139–145

Hu W, Lee KC, Cross TA (1993) Tryptophans in membrane proteins: indole ring orientations and functional implications in the gramicidin channel. Biochemistry 32:7035–7047

Kobayashi S, Chikushi A, Tougu S, Imura Y, Nishida M, Yano Y, Matsuzaki K (2004) Membrane translocation mechanism of the antimicrobial peptide buforin 2. Biochemistry 43:15610–15616

Koh JJ, Qiu S, Zou H, Lakshminarayanan R, Li J, Zhou X, Tang C, Saraswathi P, Verma C, Tan DT, Tan AL, Liu S, Beuerman RW (2013) Rapid bactericidal action of α-mangostin against MRSA as an outcome of membrane targeting. Biochim Biophys Acta 1828:834–844

Ladokhin AS, White SH (2001) 'Detergent-like' permeabilization of anionic lipid vesicles by melittin. Biochim Biophys Acta 1514:253–260

Lee JY, Yang ST, Lee SK, Jung HH, Shin SY, Hahm KS, Kim JI (2008) Salt-resistant homodimeric bactenecin, a cathelicidin-derived antimicrobial peptide. FEBS J 275:3911–3920

Lehrer RI, Barton A, Daher KA, Harwig SS, Ganz T, Selsted ME (1989) Interaction of human defensins with *Escherichia coli*. Mechanism of bactericidal activity. J Clin Invest 84:553–561

Loh B, Grant C, Hancock REW (1984) Use of the fluorescent probe 1-*N*-phenylnaphthylamine to study the interactions of aminoglycoside antibiotics with the outer membrane of *Pseudomonas aeruginosa*. Antimicrob Agents Chemother 26:546–551

Matsuzaki K (1998) Magainins as paradigm for the mode of action of pore forming polypeptides. Biochim Biophys Acta 1376:391–400

Nan YH, Bang JK, Jacob B, Park IS, Shin SY (2012) Prokaryotic selectivity and LPS-neutralizing activity of short antimicrobial peptides designed from the human antimicrobial peptide LL-37. Peptides 35:239–247

Nguyen LT, Haney EF, Vogel HJ (2011) The expanding scope of antimicrobial peptide structures and their modes of action. Trends Biotechnol 29:464–472

Oh D, Shin SY, Lee S, Kang JH, Kim SD, Ryu PD, Hahm KS, Kim Y (2000) Role of the hinge region and the tryptophan residue in the

synthetic antimicrobial peptides, cecropin A(1–8)-magainin 2(1–12) and its analogues, on their antibiotic activities and structures. Biochemistry 39:11855–11964

Ono S, Lee S, Kodera Y, Aoyagi H, Waki M, Kato T, Izumiya N (1987) Environment-dependent conformation and antimicrobial activity of a gramicidin S analog containing leucine and lysine residues. FEBS Lett 220:332–336

Oren Z, Shai Y (1998) Mode of action of linear amphipathic α-helical antimicrobial peptides. Biopolymers 47:451–463

Park CB, Kim HS, Kim SC (1998) Mechanism of action of the antimicrobial peptide buforin II: buforin II kills microorganisms by penetrating the cell membrane and inhibiting cellular functions. Biochem Biophys Res Commun 244:253–257

Park CB, Yi KS, Matsuzaki K, Kim MS, Kim SC (2000) Structure–activity analysis of buforin II, a histone H2A-derived antimicrobial peptide: the proline hinge is responsible for the cell-penetrating ability of buforin II. Proc Natl Acad Sci USA 97:8245–8250

Park K, Oh D, Shin SY, Hahm KS, Kim Y (2002) Structural studies of porcine myeloid antibacterial peptide PMAP-23 and its analogues in DPC micelles by NMR spectroscopy. Biochem Biophys Res Commun 290:204–212

Park KH, Park Y, Park IS, Hahm KS, Shin SY (2008) Bacterial selectivity and plausible mode of antibacterial action of designed Pro-rich short model antimicrobial peptides. J Pept Sci 14:876–882

Park KH, Nan YH, Park Y, Kim JI, Park IS, Hahm KS, Shin SY (2009) Cell specificity, anti-inflammatory activity, and plausible bactericidal mechanism of designed Trp-rich model antimicrobial peptides. Biochim Biophys Acta 1788:1193–1203

Sato H, Feix JB (2006) Peptide-membrane interactions and mechanisms of membrane destruction by amphipathic α-helical antimicrobial peptides. Biochim Biophy Acta 1758:1245–1256

Sawai MV, Waring AJ, Kearney WR, McCray PB Jr, Forsyth WR, Lehrer RI, Tack BF (2002) Impact of single-residue mutations on the structure and function of ovispirin/novispirin antimicrobial peptides. Protein Eng 15:225–232

Scudiero DA, Shoemaker RH, Paull KD, Monks A, Tierney S, Nofziger TH, Currens MJ, Seniff D, Boyd MR (1998) Evaluation of a soluble tetrazolium/formazan assay for cell growth and drug sensitivity in culture using human and other tumor cell lines. Cancer Res 48:4827–4833

Shin SY, Park EJ, Yang ST, Jung HJ, Eom SH, Song WK, Kim Y, Hahm KS, Kim JI (2001) Structure–activity analysis of SMAP-29, a sheep leukocytes-derived antimicrobial peptide. Biochem Biophys Res Commun 285:1046–1051

Skerlavaj B, Romeo D, Gennaro R (1990) Rapid membrane permeabilization and inhibition of vital functions of gram-negative bacteria by bactenecins. Infect Immun 58:3724–3730

Skerlavaj B, Benincasa M, Risso A, Zanetti M, Gennaro R (1999) SMAP-29: a potent antibacterial and antifungal peptide from sheep leukocytes. FEBS Lett 463:58–62

Solanas C, de la Torre BG, Fernández-Reyes M, Santiveri CM, Jiménez MA, Rivas L, Jiménez AI, Andreu D, Cativiela C (2009) Therapeutic index of gramicidin S is strongly modulated by D-phenylalanine analogues at the β-turn. J Med Chem 52:664–674

Song YM, Park Y, Lim SS, Yang ST, Woo ER, Park IS, Lee JS, Kim JI, Hahm KS, Kim Y, Shin SY (2005) Cell selectivity and mechanism of action of antimicrobial model peptides containing peptoid residues. Biochemistry 44:12094–12106

Stark M, Liu LP, Deber CM (2002) Cationic hydrophobic peptides with antimicrobial activity. Antimicrob Agents Chemother 46:3585–3590

Tack BF, Sawai MV, Kearney WR, Robertson AD, Sherman MA, Wang W, Hong T, Boo LM, Wu H, Waring AJ, Lehrer RI (2002) SMAP-29 has two LPS-binding sites and a central hinge. Eur J Biochem 269:1181–1189

Travis SM, Anderson NN, Forsyth WB, Espiritu C, Conway BD, Greenberg EB, McCray PB Jr, Lehrer RI, Welsh MJ, Tack BF (2000) Bactericidal activity of mammalian cathelicidin-derived peptides. Infect Immun 68:2748–2755

Turner J, Cho Y, Dinh N, Waring AJ, Lehrer RI (1998) Activities of LL-37, a cathelin-associated antimicrobial peptide of human neutrophils. Antimicrobial Agents Chemother 42:2206–2214

Walrant A, Vogel A, Correia I, Lequin O, Olausson BE, Desbat B, Sagan S, Alves ID (2012) Membrane interactions of two arginine-rich peptides with different cell internalization capacities. Biochim Biophys Acta 1818:1755–1763

Wiedman G, Herman K, Searson P, Wimley WC, Hristova K (2013) The electrical response of bilayers to the bee venom toxin melittin: evidence for transient bilayer permeabilization. Biochim Biophys Acta 1828:1357–1364

Wu M, Maier E, Benz R, Hancock RE (1999) Mechanism of interaction of different classes of cationic antimicrobial peptides with planar bilayers and with the cytoplasmic membrane *of Escherichia coli*. Biochemistry 38:7235–7242

Zanetti M, Gennaro R, Romeo D (1995) Cathelicidins: a novel protein family with a common proregion and a variable C-terminal antimicrobial domain. FEBS Lett 374:1–5

Zhang L, Rozek A, Hancock REW (2001) Interaction of cationic antimicrobial peptides with model membranes. J Biol Chem 276:35714–35722

Zhu WL, Hahm KS, Shin SY (2009) Cell selectivity and mechanism of action of short antimicrobial peptides designed from the cell-penetrating peptide Pep-1. J Pept Sci 15:569–575